Annals of Biomedical Engineering, Vol. 25, pp. 303–314, 1997
Printed in the USA.

0090-6964/97 $10.50 + .00

Finite Element Modeling of Drug Distribution in the Vitreous Humor of the Rabbit Eye

STUART FRIEDRICH, YU-LING CHENG, and BRADLEY SAVILLE

Department of Chemical Engineering and Applied Chemistry, University of Toronto, Toronto, Ontario, Canada

Abstract—Direct intravitreal injection of drug is a common method for treating diseases of the retina or vitreous. The stagnant nature of the vitreous humor and surrounding tissue barriers creates concentration gradients within the vitreous that must be accounted for when developing drug therapy. The objective of this research was to study drug distribution in the vitreous humor of the rabbit eye after an intravitreal injection, using a finite element model. Fluorescein and fluorescein glucuronide were selected as model compounds due to available experimental data. All required model parameters were known except for the permeability of these compounds through the retina, which was determined by fitting model predictions to experimental data. The location of the intravitreal injection in the experimental studies was not precisely known; therefore, several injection locations were considered, and best-fit retinal permeability was determined for each case. Retinal permeability of fluorescein and fluorescein glucuronide estimated by the model ranged from 1.94×10^{-5} to 3.5×10^{-5} cm s^{-1} and from 0 to 7.62×10^{-7} cm s^{-1}, respectively, depending on the assumed site of the injection. These permeability values were compared with values previously calculated from other models, and the limitations of the models are discussed. Intravitreal injection position was found to be an important variable that must be controlled in both experimental and clinical settings.

Keywords—Fluorescein, Fluorescein glucuronide, Intravitreal injection, Retinal permeability, Injection location.

INTRODUCTION

The vitreous humor is a stagnant, viscous fluid that occupies the space between the lens and retina of the eye (Fig. 1). There are a number of diseases that can affect the vitreous or the surrounding retina, which must be treated by administration of a drug. Due to physiological barriers within the eye, which prevent drug in the systemic circulation from entering the vitreous, the most common method of treating diseases affecting the vitreous or retina is a direct intravitreal injection of drug (8). Many of the drugs used have a narrow concentration range in which they are effective and may be toxic at higher concentrations (3,15–18). Knowledge of drug distribution after administration, therefore, is important if the disease is to be properly treated and damage to tissues by high concentrations of drug is to be avoided.

There have been several models developed to simulate the distribution and elimination of drugs from the vitreous (1,13,19–21). A number of other models have been used to determine the retinal permeability from the blood to the vitreous (4,7,9,10,12,14). Of the former models, the simplest approach was used by Araie and Maurice (1), who represented the vitreous as a sphere with the entire outer surface representing the retina. A more complex model was used by Yoshida *et al.* (20,21), who divided the vitreous into anterior and posterior hemispheres. Each hemisphere was further subdivided into eight compartmental shells and a separate permeability was used for the outer surface of each hemisphere. The model that most accurately duplicates the geometry and boundary conditions of the vitreous was developed by Ohtori and Tojo (13) and Tojo and Ohtori (19). The model is cylindrical in shape, with one end of the cylinder and its curved surface representing the retina, and the opposite end of the cylinder divided into an outer section representing the hyloid membrane and an inner section representing the lens. In each of these models, a simplified geometry and set of boundary and initial conditions were used so that the mathematical expression of the model would be easier to develop and solve. Some of these simplifications affect the generality of the model, and may affect model predictions and estimates of the retinal permeability.

Acknowledgment—We thank Dr. D. S. Kuhn and his research group for the use of the Silicon Graphics workstation that was used to run the FIDAP simulations. This research was supported by University of Toronto Open Doctoral Fellowships awarded to S. Friedrich, by a grant from the Whitaker Foundation (Washington, D.C.), and by a grant from the Natural Sciences and Engineering Research Council of Canada.

Address correspondence to Bradley Saville, Department of Chemical Engineering and Applied Chemistry, University of Toronto, 200 College Street, Toronto, Ontario; Canada, M5S 3E5.

(Received 28Nov95, Revised 28Mar96, Revised 21May96, Accepted 28May96)

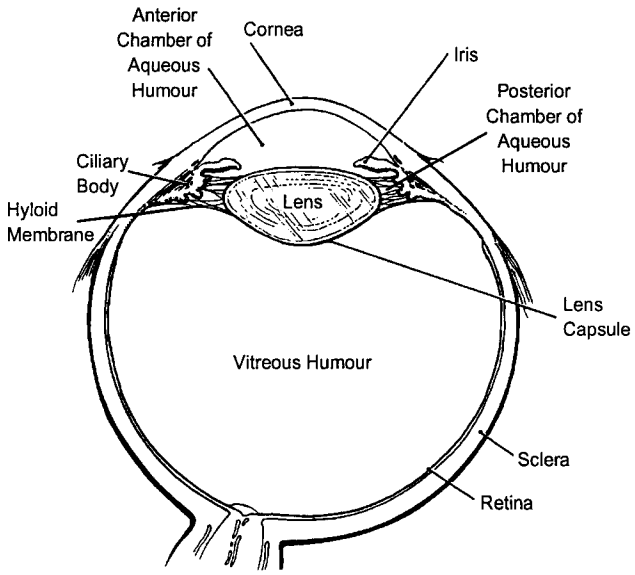

FIGURE 1. Anatomy of the human eye. The proposed model was based on the anatomy and physiology of the rabbit eye, which has a smaller vitreous volume due to a larger lens and smaller outer radius. (Adapted from 11.)

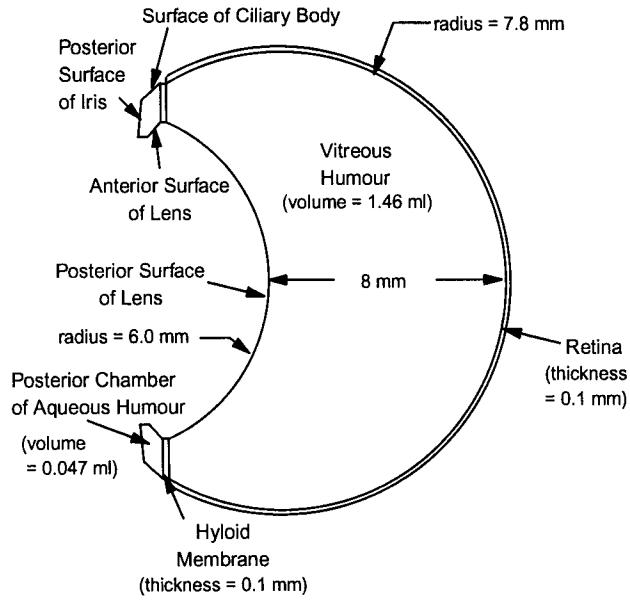

FIGURE 2. Cross-section view of the model. In addition to the vitreous, the model includes the posterior aqueous compartment and the surrounding retina layer. The aqueous compartment was included to account properly for drug loss across the hyloid membrane.

The complex geometry of the vitreous and the boundary conditions created by the tissues that surround the vitreous make this problem particularly suitable to modeling using finite element analysis. The main objective of the research described in this paper, therefore, is to develop a finite element model to describe drug distribution in the vitreous body after an intravitreal injection. Because experimental injection sites are not precisely known, it was necessary to determine the sensitivity of drug distribution to the initial location of the intravitreal injection.

MODEL DEVELOPMENT

The model was based on the physiological dimensions of a rabbit eye, using the cross-sections of the eye shown by Araie and Maurice (1) as a guide. The rabbit eye was chosen rather than the human eye because of the availability of data for confirmation of model predictions. There are three main tissues that bound the vitreous humor: the retina, lens, and hyloid membrane. The retina covers the posterior portion of the interior of the globe and is immediately adjacent to the vitreous. In a rabbit eye, the retina is supplied with nutrients via the choroid, which is the tissue layer directly outside the retina. The chloroid has a vast network of capillaries, whereas the retina is avascular. The retina is made up of several cellular layers, some of which form the blood-retinal barrier that prevents extraneous compounds from entering the vitreous from the bloodstream. The vitreous to blood permeability of the blood-retinal barrier depends on the physiocochemical properties of the drug. Some drugs cannot penetrate the barrier, whereas others may be actively transported between the vitreous and the blood. The lens forms the majority of the anterior boundary of the vitreous humor. The lens is composed of highly compacted cellular material and is therefore almost impermeable to most drugs. The hyloid membrane is composed of loosely packed collagen fibers and hyaluronic acid, and spans the gap between the lens and the ciliary body. Although the hyloid membrane forms a boundary between the stagnant vitreous and the flowing aqueous humor, it does not form a limiting barrier to the transport of small molecules such as fluorescein. The aqueous humor is continuously produced by the ciliary body and drained from the anterior chamber of the aqueous humor after it passes between the iris and the lens. Once drugs pass through the hyloid membrane, they are eliminated by the flow of aqueous humor.

Due to the difficulty in measuring concentration gradients within the vitreous, there has only been one published report that shows experimentally measured concentration profiles of model compounds across an entire cross-section of the rabbit vitreous (1). The compounds used in this study were fluorescein, fluorescein glucuronide, and fluorescein isothiocyanate. The main elimination route for fluorescein is across the retina; fluorescein glucuronide, conversely, has a very low

retinal permeability and is eliminated mainly across the hyloid membrane. Due to their different elimination characteristics, fluorescein and fluorescein glucuronide are ideal compounds for testing the model.

MODEL EQUATIONS

As described previously, drugs that pass through the hyloid membrane are eliminated by the flow of aqueous humor. A relatively small fraction of fluorescein would be eliminated across the hyloid membrane, due to its high permeability across the retina. In contrast, almost all of the fluorescein glucuronide elimination occurs across the hyloid membrane, which could then lead to a significant concentration in the aqueous humor. This was confirmed by Araie and Maurice (1), who measured concentrations of fluorescein and fluorescein glucuronide in both the aqueous and vitreous. To properly account for elimination across the hyloid, therefore, the posterior chamber of the aqueous humor was included in the model, and elimination from the anterior surface of the hyloid was determined by the flow dynamics of the aqueous humor. The choroid layer, which is situated outside the retina, is highly vascularized; therefore, a reasonable assumption is that the choroid will act as a perfect sink for drug transport across the retina. This was confirmed by a calculation that showed that, even at the maximum rate of loss of fluorescein across the retina, the flow rate of blood in the choroid results in a blood concentration that is approximately two orders of magnitude lower than the vitreous concentration next to the retina. The maximum rate of loss of fluorescein was determined by finding the maximum concentration that is present next to the retina and assuming that this concentration was the same along the entire inner surface of the retina. Figure 2 shows a cross-section view of the model that includes the dimensions of the relevant tissues of the rabbit eye. As described previously, the model dimensions were matched to those given by Araie and Maurice. Because rabbits that are used for ophthalmic research are usually of a specific size, the size of the rabbit eyes used by Araie and Maurice would have been relatively constant; therefore, the sensitivity of the model results to the dimensions of the rabbit eye was not examined.

Mass transfer in the aqueous occurs by both convective and diffusive transport. The flow velocity in the aqueous humor was determined using the Navier-Stokes equation that is shown in vector notation in Eq. 1. The flow within the aqueous was assumed to be at steady state and independent of the concentration of drug. The concentration in the aqueous was determined using the conservation of mass equation, which includes convective and diffuse terms and assumes no decomposition of drug (Eq. 2). The *Nomenclature* section describes the terms used in the equations.

$$\rho\vec{U}\cdot\nabla\vec{U} + \nabla P - \mu\nabla^2\vec{U} = 0. \quad (1)$$

$$\frac{\partial C}{\partial t} + \vec{U}\cdot\nabla C - D\nabla^2 C = 0. \quad (2)$$

Within the vitreous, hyloid, and retina, there is no fluid flow; therefore, the conservation of mass equation in these regions does not include the convective term (Eq. 3):

$$\frac{\partial C}{\partial t} - D\nabla^2 C = 0. \quad (3)$$

Initial Conditions

The initial condition that needs to be specified is the initial location and concentration of the injected fluorescein or fluorescein glucuronide within the vitreous humor at Time 0. Araie and Maurice (1) assumed that the injection was placed at the center of the vitreous humor. Due to the difficulty of locating a specific point in the vitreous when performing an injection, it is likely that the drug was not placed in the exact center of the vitreous in each case. Needle gauge, needle length, penetration angle of the needle, speed of the injection, rheology of the injected solution, and rheology of the vitreous could all affect how a drug is initially distributed in the vitreous. The position of the injected drug could affect the elimination of drug from the vitreous; therefore, rather than simulating only a central injection, four extreme injection positions were studied that cover a range of possible positions wherein the injected drug may have been placed in the *in vivo* experiments performed by Araie and Maurice: (i) a central injection, (ii) an injection placed next to the lens on the symmetry axis, (iii) an injection placed next to the retina on the symmetry axis, and (iv) an injection placed close to the hyloid membrane (Fig. 3). In the second and third cases, the injection was displaced 2 mm along the symmetry axis on either side of the midpoint between the retina and lens. In the fourth case, the injection site was displaced by 5.25 mm in a direction perpendicular to the symmetry axis and 3.25 mm in an anterior direction from the midpoint between the lens and the retina on the symmetry axis. The shape chosen to represent the injected drug solution was a cylinder of equal height and diameter (*i.e.*, the injected drug solution forms a cylinder within the vitreous immediately after the injection). Inside this cylinder, the concentration at Time 0 would be equal

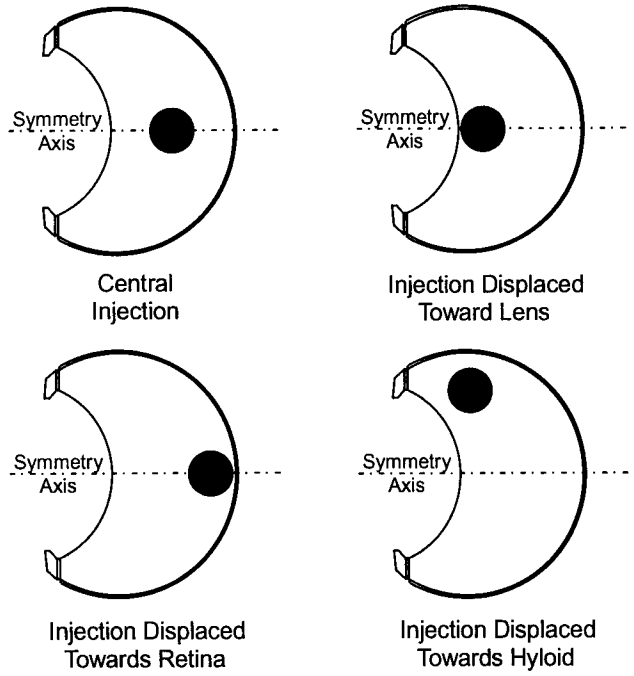

FIGURE 3. Injection positions studied using the model. Four distinct injection positions were studied to determine the sensitivity of the model-calculated retinal permeability to the initial location of the injected drug.

to the concentration of drug that was injected, and outside the cylinder, the concentration would be zero. The cylindrical shape was chosen rather than a sphere to simplify the creation of the finite element mesh within the model. The sensitivity of drug distribution to the shape of the injected drug will be discussed in *Results*. The injection volume used by Araie and Maurice for both fluorescein and fluorescein glucuronide was 15 μl, and the concentrations were 2 mg ml^{-1} and 1.7 mg ml^{-1}, respectively.

Boundary Conditions

Because the vitreous is symmetrical about an axis that passes through the center of the lens and the vitreous, only a fraction of the vitreous and aqueous needed to be modeled. The fraction that was modeled depended on the placement of the injection. The boundary conditions, vitreous, and injected drug are all symmetrical about the same axis for the lens displaced, retina displaced and central injection cases; therefore, only a small section (1/20th) of the whole vitreous was modeled (Fig. 4). Although a two-dimensional, axisymmetric model would have sufficed for these three injection locations, a three-dimensional section was modeled so that all of the models would have the same configuration. For the injection that was displaced toward the hyloid membrane, half of the vitreous was modeled, with the symmetry plane passing through the middle of both the injection and the vitreous (Fig. 5).

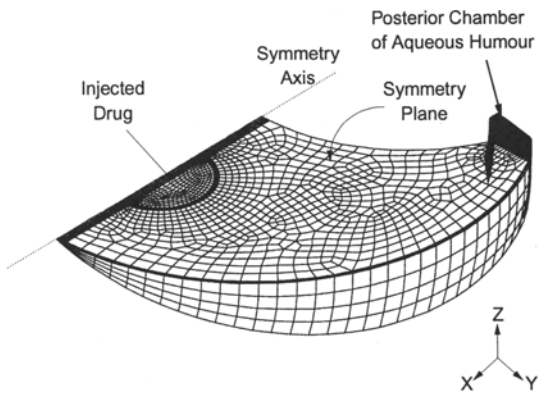

FIGURE 4. Finite element distribution for spherical central injection. The finite element mesh was created by first pave-meshing one of the symmetry surfaces and then map-meshing this surface around the symmetry axis. In this case, only 1/20th of the entire vitreous was modeled due to symmetry. For the lens-displaced injection and retina-displaced injection cases, the mesh is very similar except for the location of the injected drug.

Four boundary conditions were defined for the aqueous humor flow dynamics. The fluid velocity at the surface of the iris and at the anterior surface of the lens was set at zero (Eq. 4). The ciliary body produces the aqueous fluid, so the fluid velocity was calculated from the rate of production of aqueous fluid [2.2×10^{-3} ml min^{-1} (4)] and the area of the ciliary body boundary (0.41 cm^2). The aqueous fluid was as-

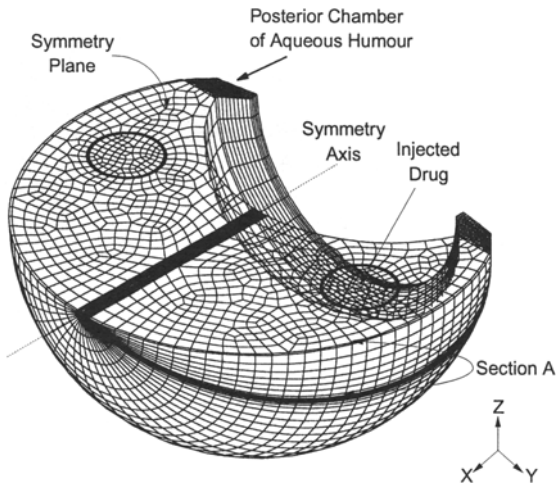

FIGURE 5. Finite element distribution for hyloid-displaced injection. In this injection case, the injected drug is not located on the symmetry axis; therefore, half of the vitreous was modeled with the symmetry plane bisecting both the injection and the vitreous. Note that the injected drug is only contained within Section A shown on the diagram.

sumed to flow in a normal direction with respect to the surface of the ciliary body (Eq. 5) and, consequently, the two tangential velocity components were set equal to zero (Eq. 6). At the symmetry surfaces of the aqueous, where the model was sectioned, the velocity normal to the surface was set equal to zero (Eq. 7). This assumes that aqueous is produced and eliminated at a uniform rate around the posterior aqueous humor compartment. Because the flow dynamics within the posterior aqueous humor can be completely defined using velocity boundary conditions, pressures can be calculated with respect to a reference pressure at one point.

$$\vec{U} = 0 \text{ @ tissue surfaces} \quad (4)$$

$$U_n = 9 \times 10^{-5} \text{ cm s}^{-1} \text{ @ aqueous next to ciliary body} \quad (5)$$

$$U_{t1} \text{ and } U_{t2} = 0 \text{ @ aqueous next to ciliary body} \quad (6)$$

$$U_n = 0 \text{ @ symmetry surfaces of aqueous} \quad (7)$$

At the surface of the lens, and at all the symmetry surfaces, a no-flux boundary condition was applied (Eq. 8), and, because the blood is a perfect sink, the concentration at the outer surface of the retina could be set equal to zero (Eq. 9).

$$\frac{\partial C}{\partial n} = 0 \text{ @ lens surface and symmetry surfaces} \quad (8)$$

$$C = 0 \text{ @ outer surface of retina} \quad (9)$$

The parameters required to solve the model are flow rate, viscosity and density of the aqueous humor, diffusivity of the vitreous, and permeability of the retina. Of these five parameters, only the permeability of the retina must be estimated using the model. The remaining four were known based on previous experiments or on physical properties of the model drugs. The velocity within the aqueous next to the ciliary body, used as a boundary condition to determine the aqueous humor velocity profile, was calculated using the production rate of aqueous humor in the rabbit eye. A viscosity of 6.9×10^{-3} g cm^{-1} s^{-1} and a density of 1 g cm^{-3} were used, because the fluid properties of the aqueous are essentially identical to that of water. Although the vitreous and hyloid membrane contain hyaluronic acid and collagen, the concentration of these components is very low. Therefore, the diffusivity of small molcules, such as fluorescein and fluorescein glucuronide in the vitreous and hyloid membrane, is essentially the same as in an aqueous solution [6×10^{-6} cm^2 s^{-1} (1)]. Using an empirical relationship developed by Davis (2) for calculating the diffusivity of molecules in a hydrogel, it can be shown that, for the diffusivity in the vitreous or hyloid membrane to decrease by 50%, the concentration of collagen and hyaluronic acid that is normally present would have to increase by a factor of 400, which is not possible physiologically.

The retinal permeability of fluorescein and fluorescein glucuronide has been previously determined by fitting model-predicted concentrations and experimental concentrations (1,20,21). However, the reported permeability values may be inaccurate due to the simplifying assumptions made in the models and the uncertainty of the injection position. In this work, we endeavor to predict retinal permeability using a model based on the actual physiology of the eye, with a minimum of simplifying assumptions. There are two unknown variables in this model: the initial position of the injected drug and retinal permeability; both of these factors directly influence the rate of drug elimination and concentration profiles in the vitreous. Retinal permeability is a constant for a specific drug and will not change unless there is a physiological change in the retina. In the ideal situation, injection position would be known precisely, and a unique, physiologically accurate value for retinal permeability could be predicted using experimentally measured concentration profiles. However, because the exact injection location in Araie and Maurice's (1) experiments are not known and different injection positions were assumed in this study, retinal permeability values that correspond to each assumed injection position were found. By choosing extreme injection positions, the range of retinal permeabilities predicted by the model should cover a range that includes the actual physiological retinal permeability. These retinal permeability values will be compared with other published values.

Although the model can calculate the concentration of fluorescein or fluorescein glucuronide at any point within the vitreous, model predicted concentrations were fit to the experimental data collected by Araie and Maurice at only the point immediately adjacent to the lens on the symmetry axis of the vitreous. This limited fitting was done for several reasons. A more rigorous fitting was limited by the quantity of experimental data reported by Araie and Maurice. Experimental concentration profiles were collected only at 15 hr for fluorescein and at 24 hr for fluorescein glucuronide. For fluorescein, these data were presented in two ways: a single concentration contour profile that showed the absolute concentration values for an entire cross-section of a typical eye, and a plot that showed the average normalized concentration profile along the symmetry axis between the lens and the retina for

eight eyes. For fluorescein glucuronide, concentrations at the lens and retina on the symmetry axis were found to be equal; therefore, a normalized concentration profile between the lens and retina for the eight eyes was not shown. The reference concentration that was used to produce the normalized profile of fluorescein was not reported; therefore, the only way to obtain average absolute concentrations of fluorescein between the lens and retina for all eight eyes would be to correlate the normalized profile of fluorescein to the absolute concentration of fluorescein reported at one point of the typical eye. However, this assumes that the absolute concentration at the selected point of the typical eye adequately represents the average for all eight eyes. Even if this assumption was valid, fitting the model predicted concentrations to the experimental data at a large number of points within the vitreous would be very computationally intensive. Calculations of the residual between the model-predicted data and the experimental data would have to be done separately after each finite element model simulation, and retinal permeability would be adjusted manually until the residual was minimized. Furthermore, because the normalized data of Araie and Maurice do not indicate the mean ± SD, but rather a range, the error in each data point could not be determined, and a full scale fit could not be justified. Finally, matching the model-predicted concentrations to only one point of the experimental data, while allowing the model to calculate the concentrations in the rest of the vitreous, would also test the robustness of the model.

FINITE ELEMENT ANALYSIS

The fraction of the vitreous and aqueous described previously was divided into a number of brick elements that were defined by eight corner nodal points. Equations 1 to 3, which describe fluid mechanics and mass transport within the eye, are replaced by ordinary differential equations for transient analysis and algebraic equations for steady-state analysis. This system of equations has matrix coefficients that are derived by approximating the continuum equations on each element. The resulting nonlinear system of equations is then solved to determine the degree(s) of freedom of the model (velocity components or concentration) at each node of every element.

FIDAP (Fluid Dynamics International, Inc., Evanston, IL, USA) was used to perform the finite element analysis, and simulations were run on a Silicon Graphics Iris workstation. Approximately 9,000 finite elements were used for the cases where the injection was placed on the symmetry axis of the vitreous, whereas the hyloid-displaced injection case used 40,000 elements. Figures 4 and 5 show the element distribution for the spherical central injection case and the hyloid displaced injection case, respectively. The smallest elements were needed at the boundary around the site of injection because, at Time 0, there would be a very steep concentration gradient between the injection site and the surrounding vitreous. Small elements were also used within the aqueous to ensure that the fluid velocity profile was calculated accurately, and within the retina due to the higher concentration gradients expected across the retina. The velocity profile within the aqueous was solved independently of the drug distribution problem, and this solution was used in the simulations that solved the mass-transport portion of the problem. The time required to simulate 24 hr in real time ranged from ~1 hr for the injections located on the symmetry axis to 5 hr for the hyloid-displaced injection.

Sensitivity of the model results to the element mesh configuration was studied during the creation of the models by examining the solution residual at each node at each time step. The final element mesh used for each model produced solution residuals that ranged from 0.01 to 0.1, which is within the range recommended by FIDAP. The shape of the elements was also optimized for each model by ensuring that their aspect ratio and distortion were within recommended guidelines. When developing the mesh, the first step is to define the lines that bound the model, and define the number and distribution of nodes on these lines. After this, the three-dimensional mesh was developed by first pave-meshing the symmetry plane that is defined by the boundary lines, which includes the inner region that defines the injected drug, and then projecting this two-dimensional mesh along a curved line using a mapped mesh. Pave-meshing refers to an automatic mesh generation routine the can be used to mesh an irregular two-dimensional area. Mapped meshing is used when the area or volume to be meshed has lines or sides that can be uniquely mapped to a second line or side of the model.

SIMULATION RESULTS AND DISCUSSION

Figure 6 shows the model predicted velocity profile within the aqueous humor as both a contour plot (A) and a vector plot (B) on a cross-section of the aqueous humor. As expected, the velocity increases as the gap between the lens and the iris grows smaller.

Figures 7 and 8 show the model-predicted concentration profiles for fluorescein at 15 hr and for fluorescein glucuronide at 24 hr, respectively, after a spherical central injection (A) and a cylindrical injection displaced toward the hyloid membrane (B). Concentra-

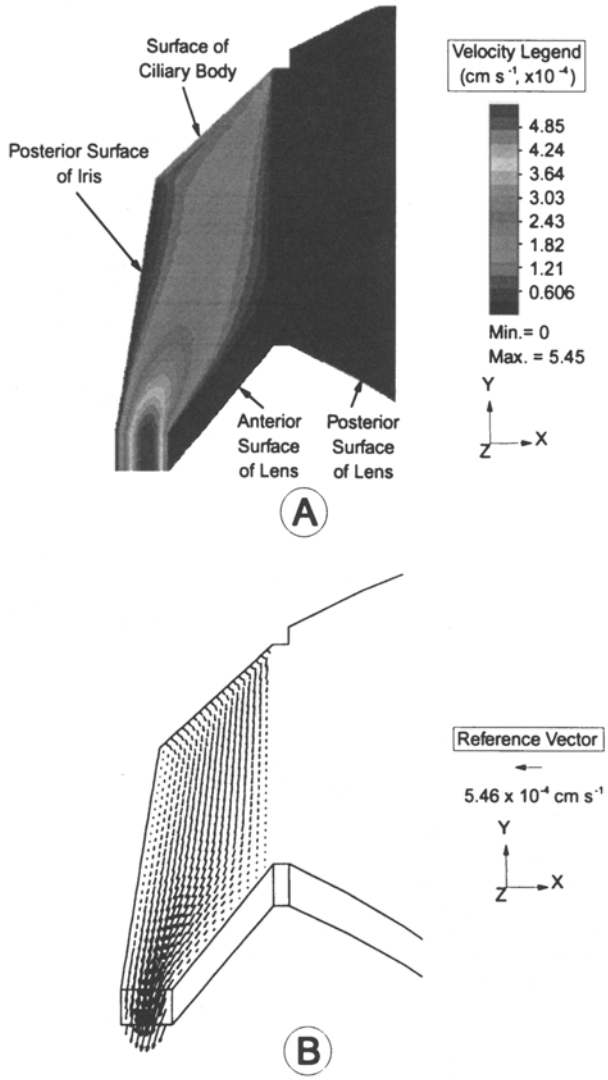

FIGURE 6. Contour plot (A) and vector plot (B) of the model-predicted velocity profile within the posterior aqueous humor. The aqueous is produced by the ciliary body and passes between the lens and iris. The highest fluid velocities were found where the gap between the lens and the iris is the smallest. Fluid velocities at the tissue surfaces were assumed to be zero.

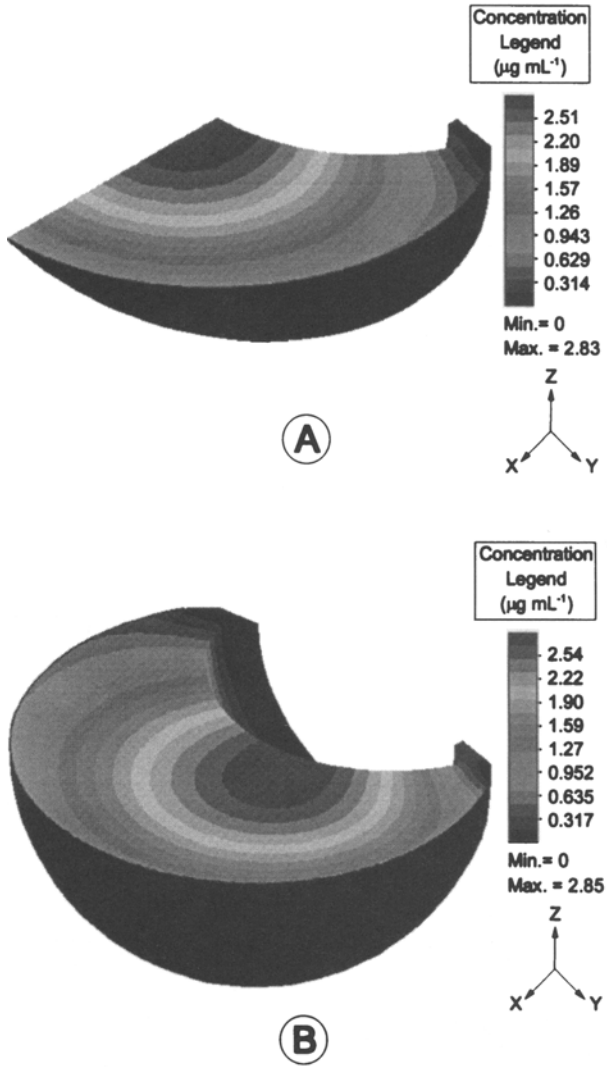

FIGURE 7. Model-predicted concentration profile for fluorescein at 15 hr for a spherical central injection (A) and a hyloid-displaced injection (B). The dominant elimination route for fluorescein is across the retina; therefore, concentration contour lines are parallel to the retina surface. The concentration profile for the lens-displaced injection and the retina-displaced injection was qualitatively similar to the central injection.

tion profiles for the cylindrical central injection, the cylindrical injection displaced toward the lens, and the cylindrical injection displaced toward the retina were qualitatively similar to the concentration profile produced by the spherical central injection. Qualitatively, the contour profiles found using the model are similar to those found experimentally by Araie and Maurice (1). In Fig. 7, the concentration contour lines are parallel to the retina as expected, because the flux of fluorescein across the retina was the dominant elimination mechanism. For each injection position along the symmetry axis, the maximum model-predicted concentrations were next to the lens, on the symmetry axis as in Fig. 7A. In the case where fluorescein was injected closer to the hyloid membrane (Fig. 7B), the maximum model-predicted concentration was next to the lens; however, it is displaced slightly closer to the site of the injection.

In Fig. 8, the model-predicted concentration contour lines are perpendicular to the retina, because fluorescein glucuronide is eliminated mainly across the hyloid membrane. Araie and Maurice found that the concentration of fluorescein glucuronide in the vitreous was approximately the same next to the retina and next to the lens on the symmetry axis of the vitreous at 24 hr. However, the model predicted that the con-

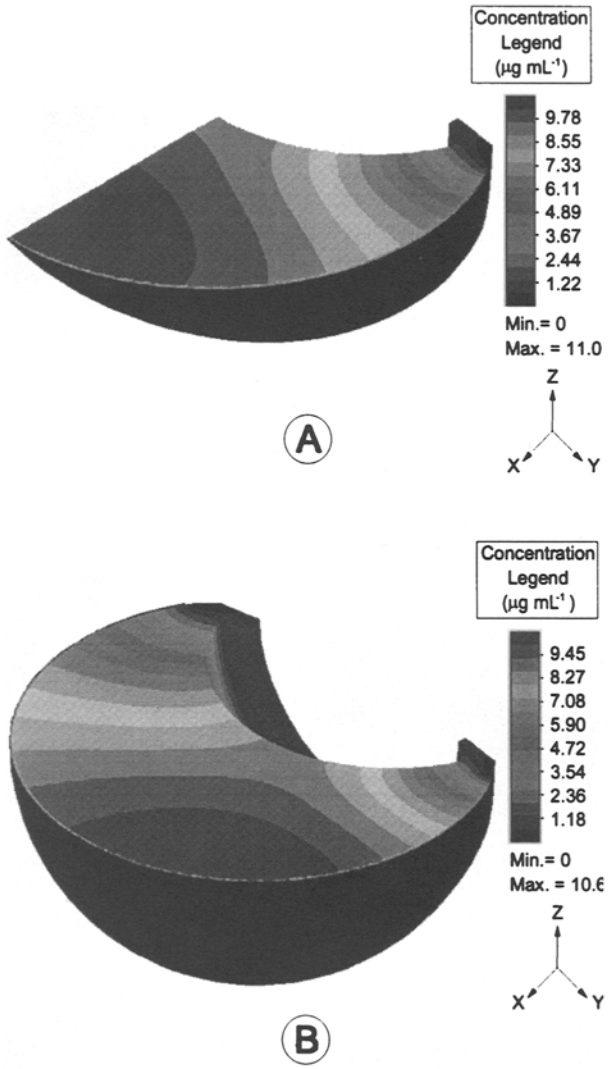

FIGURE 8. Model-predicted concentration profile for fluorescein glucuronide at 24 hr for a spherical central injection (A) and a hyloid-displaced injection (B). Fluorescein glucuronide has a very low retinal permeability; therefore, concentration contour lines are perpendicular to the retina. The concentration profile for the lens-displaced injection and the retina-displaced injection was qualitatively similar to the central injection.

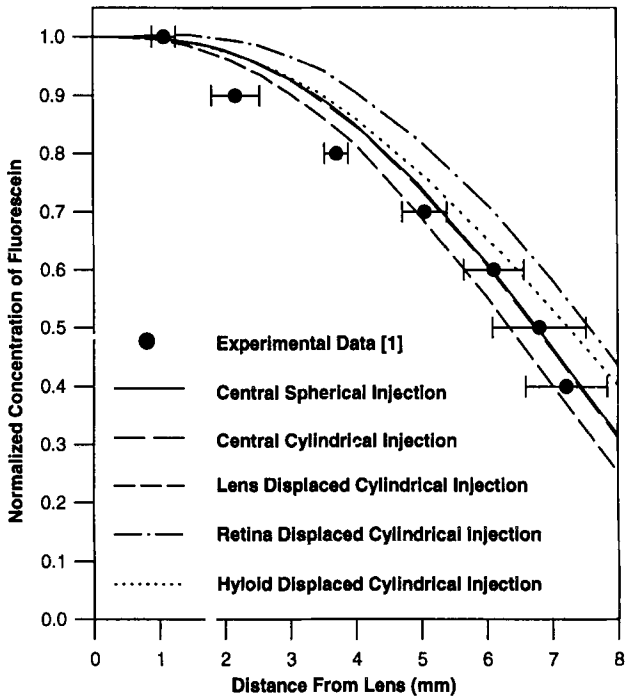

FIGURE 9. Concentration gradient between the lens and retina, 15 hr after an intravitreal injection of fluorescein. Concentrations have been normalized with respect to the concentration next to the lens. Experimental bars represent the minimum and maximum distances from the center of curvature of the retina that each specific experimental concentration contour line was observed (1). Model-predicted profiles were produced using the retinal permeabilities shown in Table 1. Retinal permeabilities were predicted by fitting only the experimental concentration next to the lens. However, the model was able to predict the entire profile accurately.

centration next to the retina (12.1 μg ml^{-1}) is slightly higher than the concentration next to the lens (10.4 μg ml^{-1}) for all injection positions. For the hyloid-displaced injection, the maximum concentration was shifted slightly toward the injection site, similar to what was noted for the hyloid-displaced injection of fluorescein. If the hyloid membrane was the only elimination route, theory would suggest that the maximum concentration would be next to the retina on the symmetry axis, because this is the point where a drug molecule must travel furthest to be eliminated.

In Fig. 9, the model-predicted concentration gradients of fluorescein between the lens and the retina along the symmetry axis are compared with the experimental data of Araie and Maurice. In each case, concentrations have been normalized with respect to the concentration found next to the lens. Considering that the model gradients were calculated by matching only the experimental concentration next to the lens, the fact that all the model-predicted gradients follow the experimentally observed gradient provides strong validation of the model and its inherent assumptions. Of particular note is that even 15 hr after the intravitreal injection, significant variations were observed when different injection locations were considered. At earlier times after the injection, the concentration variations would be much larger, which suggests that injection position is an important variable that must be controlled when performing experiments or when injecting drugs into patients.

Table 1 shows, for each of the simulated injection positions, the retinal permeabilities of fluorescein and

TABLE 1. Comparison of model-calculated retinal permeabilities and other published values

Position of Injection and Other Published Values	Retinal Permeability ($cm\ s^{-1}$)	
	Fluorescein	Fluorescein Glucuronide
Central spherical injection	2.88×10^{-5}	6.41×10^{-7}
Central cylindrical injection	2.88×10^{-5}	6.41×10^{-7}
Injection displaced toward lens	3.50×10^{-5}	3.89×10^{-7}
Injection displaced toward retina	2.03×10^{-5}	7.62×10^{-7}
Injection displaced toward hyloid membrane	1.94×10^{-5}	0
Araie and Maurice (1)	2.33×10^{-5}	Not calculated
Koyano *et al.* (6)	0.6×10^{-5} to 1.8×10^{-5}	6.3×10^{-6}
Yoshida *et al.* (20,21)[a]	1.27×10^{-5}	1.5×10^{-6}

[a]These data were collected for monkey eyes, but were included for comparison.

fluorescein glucuronide that were found to match the experimental data best, and compares them with values predicted by other published models, and that were found *in vitro* by Koyano *et al.* (6) using an excised rabbit retina. As mentioned previously, retinal permeability for a compound is a constant. Different values obtained from the various simulations occur because retinal permeability is the only free parameter that may be adjusted to predict experimental data. Because the injection position affects the concentration gradients in the vitreous, different estimates of the permeabilities are obtained. Retinal permeabilities calculated for a central spherical injection and a central cylindrical injection were the same. This confirms that the use of a cylindrical injection shape to simplify the creation of the finite element mesh was valid. Estimated fluorescein retinal permeabilities were much lower when the injection was displaced toward the retina or the hyloid membrane. In the former case, fluorescein was placed closer to the retina, producing a higher initial concentration gradient of fluorescein across the retina than obtained from a central injection. Since the concentration gradient is higher, a lower retinal permeability is required to fit the experimental data. In the latter case, the injection position is closer to both the retina and the hyloid membrane than with a central injection. Retinal penetration is the dominant elimination mechanism for fluorescein; however, when the injection is placed closer to the hyloid membrane, more fluorescein will be eliminated across the hyloid membrane than if the injection was placed in the center of the vitreous. The combination of a greater loss across the hyloid membrane and a higher initial concentration gradient across the retina results in a lower retinal permeability required to match the experimental data. Displacement of the injection toward the lens led to the highest estimate of the retinal permeability, because this injection position places fluorescein furthest from the retina, compared with the other three injection positions.

A retinal permeability of zero was obtained when the injection of fluorescein glucuronide was displaced toward the hyloid membrane. A low retinal permeability is expected, because penetration across the hyloid membrane is the main elimination route for fluorescein glucuronide, and an injection placed closer to the hyloid membrane will increase the amount of fluorescein glucuronide eliminated across the hyloid membrane. Therefore, a lower retinal permeability will be required to fit the experimental data. Because fluorescein glucuronide is known to penetrate the retina and the model has estimated a retinal permeability of zero, it is reasonable to conclude that the extreme position of the hyloid displaced injection is significantly different than the actual experimental injection position, thus leading to an error in the estimation of the retinal permeability. This result is also due to the low sensitivity of the fluorescein glucuronide concentration at 24 hr to retinal permeability. For the other three injection positions, as the injection site is moved further from the hyloid membrane, the net elimination across the hyloid is reduced. To compensate, the simulated amount of drug transferred across the retina must increase, and, therefore, the estimated retinal permeability increases as the injection site is placed further from the hyloid membrane.

Retinal permeability of fluorescein predicted by the models of Araie and Maurice and Yoshida *et al.* (20,21) and found *in vitro* by Koyano *et al.* are close to the range of retinal permeabilities predicted by the model. As described in the *Introduction,* Araie and Maurice assumed that the vitreous could be adequately represented by a sphere, where the entire surface of the sphere represented the retina (Fig. 10). The concentration profile calculated by this model would be the same for any cross-section that passes through the center of

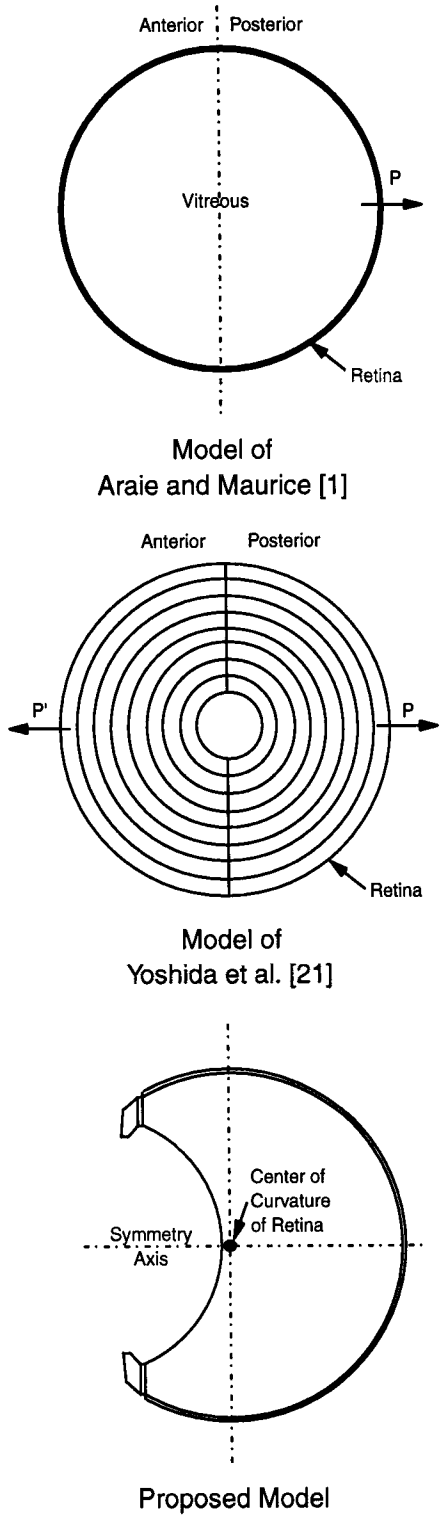

FIGURE 10. Comparison of models developed by Araie and Maurice (1) and Yoshida *et al.* (21) to the proposed model. The proposed model has a geometry and boundary conditions that more accurately reflect the true conditions present in the eye and allows a more accurate prediction of drug distribution.

the sphere, with the highest concentration in the center and the lowest concentration next to the outer surface. In a rabbit eye, the center of curvature of the retina is immediately next to the lens, on the symmetry axis of the vitreous. Qualitatively, the concentration profile calculated by a spherical model will be correct for the posterior hemisphere of the vitreous that is behind the center of curvature of the retina. In a spherical geometry, the concentration profile in the anterior hemisphere will be the same as the posterior hemisphere, because the two hemispheres are the same. The concentration profile based on a spherical model for the portion of the vitreous that is in front of the center of curvature of the retina, therefore, will not accurately reflect the actual profile that would be present. A spherical model also assumes that there is no flux across the plane that passes through the center of curvature of the retina and is perpendicular to the symmetry axis. For this assumption to be true, the loss across the retina that is behind the center of curvature of the retina must equal the sum of the loss across the hyloid membrane and the loss across the retina in front of the center of curvature of the retina. This condition will only be true for a particular retinal permeability. The fluorescein retinal permeability calculated by Araie and Maurice agrees with the retinal permeability calculated with our model. Therefore, this permeability value is coincidentally the value that is required to balance the anterior and posterior losses. Retinal permeability calculated with a spherical model for any compound that does not have an actual retinal permeability similar to fluorescein, therefore, will be in error.

Yoshida *et al.* used their model to calculate retinal permeability of fluorescein and fluorescein glucuronide in monkey eyes, which means that any differences between the retinal permeability calculated by their model and the proposed model could be due to differences between the models and also due to differences between the physiology of the rabbit and monkey retina. However, a comparison of the two models on a theoretical basis can still be made. Yoshida *et al.* divided the vitreous into anterior and posterior hemispheres. Each hemisphere was further subdivided into eight compartmental shells, and a separate permeability was used for the outer surface of each hemisphere. Within each concentric compartmental shell, the concentration calculated by the model would be uniform, because each compartment is assumed to be perfectly mixed. As noted experimentally by Araie and Maurice, and with our model, the concentration contours of fluorescein form concentric rings that are parallel to the retina in the rabbit eye. Concentration contours in a monkey eye would be similar due to the high permeability of fluorescein through the monkey retina.

Concentration contours calculated using Yoshida's model for the posterior portion of the vitreous, therefore, would be qualitatively correct. Because the anterior portion of Yoshida's model is also defined by concentric compartmental shells and the concentration contours in the region close to the hyloid membrane are not parallel to the retina, the concentration profile calculated for the anterior portion of the vitreous would be incorrect. Yoshida's model is a more accurate representation of the true vitreous than a spherical model, because a separate permeability is calculated for the outer surface of the anterior and posterior hemispheres. However, an accurate estimate of retinal permeability will only be obtained for compounds that are primarily eliminated across the retina. Compounds that are eliminated mainly across the hyloid membrane will have concentration contours that are perpendicular to the retina and, therefore, the concentric compartmental shells will not accurately predict the correct concentration profile. The profile predicted by a model that uses concentric compartmental shells will always have concentration contours that are parallel to the retina, because the concentration within each compartmental shell must be uniform. Furthermore, because the concentration in the vitreous (adjacent to the retina) calculated by a concentric shell compartmental model will be always be uniform over the entire inner surface of the retina, the model will be unable to account for conditions that result in nonuniform concentrations adjacent to the retina.

Although the retinal permeability of fluorescein found *in vitro* by Koyano *et al.* is similar to the values found using the proposed model, the retinal permeability of fluorescein glucuronide that was found is significantly different than the value found using the proposed model. To test the value that was found by Koyano *et al.*, a model simulation was performed using their permeability value and a central injection of fluorescein glucuronide with the same injected concentration used by Araie and Maurice. As described previously, concentration contour lines of fluorescein glucuronide were found to be perpendicular to the retina at 24 hr experimentally by Araie and Maurice and by the proposed model for any of the injection positions. When the retinal permeability value found be Koyano *et al.* was used in the model, however, the concentration contour lines at 24 hr were found to be parallel to the retina, very similar to the profiles for fluorescein. If the profiles found experimentally by Araie and Maurice are assumed to be correct, then it must be concluded that the retinal permeability values found *in vitro* by Koyano *et al.* are not accurate. This may be due to the difficulty of excising a retina from the eye and maintaining its viability while permeation experiments are performed.

With our model, we have analyzed the effects of injections placed at extreme positions within the vitreous. The actual position and shape of an intravitreal injection will most likely not be the same as any of these assumed conditions; however, the model results have indicated the variability that can occur when the injection is not placed in the same position each time. Not only is knowledge of the actual injection position and shape required to calculate the correct retinal permeability, it is also very important for calculating the correct concentrations within the vitreous. Different injection positions and shapes will produce different concentrations within the vitreous and, therefore, the quality of the treatment afforded by the drug will change.

CONCLUSIONS

A finite element model has been developed and shown to accurately predict drug distribution within the vitreous humor. Using the finite element model of the vitreous, we have shown that the site of an intravitreal injection has a substantial effect on drug distribution and elimination in the vitreous. Retinal permeability of fluorescein and fluorescein glucuronide calculated by the model ranged from 1.94×10^{-5} to 3.5×10^{-5} cm s^{-1} and from 0 to 7.62×10^{-7} cm s^{-1}, respectively, depending on the assumed site of the injection. The actual physiological retinal permeability will be a constant that should lie within these ranges. If the exact initial location and distribution of the drug were known, the model would be able to calculate the actual, unique, retinal permeability. Future plans include modifying the model to match the geometry of the human eye and studying the effect of different injection positions, and conditions such as aphakia and a breakdown of the blood-retinal barrier, on concentrations within the vitreous.

REFERENCES

1. Araie, M., and D. M. Maurice. The loss of fluorescein, fluorescein glucuronide and fluorescein isothiocyanate dextran from the vitreous by the anterior and retinal pathways. *Exp. Eye Res.* 52:27–39, 1991.
2. Davis, B. K. Diffusion in polymer gel implants. *Proc. Natl. Acad. Sci U.S.A.* 71:3120–3123.
3. Forster, R. K., R. L. Abbott, and H. Gelender. Management of infectious endophthalmitis. *Ophthalmology* 87:313–319, 1980.
4. Hosaka, A. Permeability of the blood-retinal barrier in myopia. An analysis employing vitreous fluorophotometry and computer simulation. *Acta Ophthalmol. Suppl.* 185:95–99, 1988.

5. Kinsey, V. E., and D. V. N. Reddy. Chemistry and dynamics of aqueous humor. In: The rabbit eye in research, edited by J. H. Prince. Springfield: C. C Thomas, 1964, pp. 218–319.
6. Koyano, S., M. Araie, and S. Eguchi. Movement of fluorescein and its glucuronide across retinal pigment epithelium-choroid. *Invest. Ophthalmol. Vis. Sci.* 34: 531–538, 1993.
7. Larsen, J., H. Lund-Andersen, and B. Krogsaa. Transient transport across the blood-retina barrier. *Bull. Math. Biol.* 45:749–758, 1983.
8. Lee, V. H. L., K. J. Pince, D. A. Frambach, *et al.* Drug delivery to the posterior segment. In: Retina, edited by T. E. Ogden and A. P. Schachat. St. Louis: C. V. Mosby, 1989, pp. 483–498.
9. Lund-Andersen, H., B. Krogsaa, M. la Cour, and J. Larsen. Quantitative vitreous fluorophotometry applying a mathematical model of the eye. *Invest. Ophthalmol. Vis. Sci.* 26:698–710, 1985.
10. Lund-Andersen, H., B. Krogsaa, and J. Larsen. Calculation of the permeability of the blood-retinal barrier to fluorescein. *Graef. Arch. Clin. Exp. Ophthalmol.* 222: 173–176, 1985.
11. McDonnell, J. H. Ocular embryology and anatomy. In: Retina: basic science, inherited retinal disease, and tumors, vol. 1, edited by T. E. Ogden, St. Louis: C. V. Mosby Company, 1989, pp. 1–12.
12. Ogura, Y., Y. Tsukahara, I. Saito, and T. Kondo. Estimation of the permeability of the blood-retinal barrier in normal individuals. *Invest. Ophthalmol. Vis. Sci.* 26:969–976, 1985.
13. Ohtori, A., and K. Tojo. In vivo/in vitro correlation of intravitreal delivery of drugs with the help of computer simulation. *Biol. Pharm. Bull.* 17:283–290, 1994.
14. Palestine, A. G., and R. F. Brubaker. Pharmacokinetics of fluorescein in the vitreous. *Invest. Ophthalmol. Vis. Sci.* 21:542–549, 1981.
15. Pflugfelder, S. C., E. Hernandez, S. J., Fliesler, J. Alvarez, M. E. Pflugfelder, and R. K. Forster. Intravitreal vancomycin. Retinal toxicity, clearance, and interaction with gentamicin. *Arch. Ophthalmol.* 105:831–837, 1987.
16. Stainer, G. A., G. A. Peyman, H. Meisels, and G. Fishman. Toxicity of selected antibiotics in vitreous replacement fluid. *Ann. Ophthalmol.* 9:615–618, 1977.
17. Tabatabay, C. A., D. J. D'Amico, L. A. Hanninen, and K. R. Kenyon. Experimental drusen formation induced by intravitreal aminoglycoside injection. *Arch. Ophthalmol.* 105:826–830, 1987.
18. Talamo, J. H., D. J. D'Amico, L. A. Hanninen, K. R. Kenyon, and E. T. Shanks. The influence of aphakia and vitrectomy on experimental retinal toxicity of aminoglycoside antiobiotics. *Am. J. Ophthalmol.* 100: 840–847, 1985.
19. Tojo, K., and A. Ohtori. Pharmacokinetic model of intravitreal drug injection. *Math. Biosci.* 12359–12375, 1994.
20. Yoshida, A., S. Ishiko, and M. Kojima. Outward permeability of the blood-barrier barrier. *Graef. Arch. Clin. Exp. Ophthalmol.* 230:78–83, 1992.
21. Yoshida, A., M. Kojima, S. Ishiko, *et al.* Inward and outward permeability of the blood-retinal barrier. In: Ocular fluorophotometry and the future, edited by J. Cunha-Vaz and E. Leite. Amsterdam: Kugler & Ghedini Publishers, 1989, pp. 89–97.

NOMENCLATURE

C = concentration of drug (g ml^{-1})
D = diffusivity (cm^2 s^{-1})
P = pressure (g cm^{-1} s^{-2} or μPa)
t = time (sec)
$\vec{U}$ = velocity vector (cm s^{-1})
μ = viscosity (g s^{-1} cm^{-1})
ρ = density (g cm^{-3})
∇ = grad (vector operator)
$\cdot$ = dot product (vector operator)

Subscripts

n = normal direction
t1,t2 = tangential directions